Available online at www.sciencedirect.com
ScienceDirect
Journal of Power Sources 163 (2007) 1064–1069
JOURNAL OF POWER SOURCES
www.elsevier.com/locate/jpowsour

Short communication

Surfactant based sol–gel approach to nanostructured $LiFePO_4$ for high rate Li-ion batteries

Daiwon Choi [a], Prashant N. Kumta [a,b,*]

[a] *Department of Materials Science and Engineering, Carnegie Mellon University, Pittsburgh, PA 15213, United States*
[b] *Department of Biomedical Engineering, Carnegie Mellon University, Pittsburgh, PA 15213, United States*

Received 6 September 2006; received in revised form 25 September 2006; accepted 26 September 2006
Available online 17 November 2006

Abstract

Porous nanostructured $LiFePO_4$ powder with a narrow particle size distribution (100–300 nm) for high rate lithium-ion battery cathode application was obtained using an ethanol based sol–gel route employing lauric acid as a surfactant. The synthesized $LiFePO_4$ powders comprised of agglomerates of crystallites <65 nm in diameter exhibiting a specific surface area ranging from 8 $m^2\,g^{-1}$ to 36 $m^2\,g^{-1}$ depending on the absence or presence of the surfactant. The $LiFePO_4$ obtained using lauric acid resulted in a specific capacity of 123 mAh g^{-1} and 157 mAh g^{-1} at discharge rates of 10*C* and 1*C* with less than 0.08% fade per cycle, respectively. Structural and microstructural characterization were performed using X-ray diffraction (XRD), scanning electron microscopy (SEM) and high-resolution transmission electron microscopy (HRTEM) with energy dispersive X-ray (EDX) analysis while electronic conductivity and specific surface area were determined using four-point probe and N_2 adsorption techniques.

Keywords: Lithium-ion battery; Cathode; $LiFePO_4$; Surfactant; Sol–gel approach

1. Introduction

There is an ever-increasing demand for batteries exhibiting higher energy and power densities due to the continued growing energy storage needs for current and future portable electronic devices and electrical vehicles [1–3]. In this regard, olivine structured $LiFePO_4$ proposed by Goodenough and co-workers have attracted much interest due to the low cost, low toxicity and theoretical capacity of 170 mAh g^{-1} with a flat discharge–charge potential at 3.45 V versus Li/Li^+ owing to the Fe^{2+}/Fe^{3+} redox couple [1,4]. Also, the high stability of the $LiFePO_4$ host lattice with minimal changes in the unit cell parameters during the $LiFePO_4/FePO_4$ phase transition are recognized as the contributing factors promoting the good cycle life of the system [5]. However, due to the low intrinsic electronic conductivity (10^{-8} to 10^{-10} S cm^{-1}) of $LiFePO_4$, it is difficult to utilize the full theoretical capacity at useful rates [1,6]. Consequently, extensive research has been conducted in recent years to improve its conductivity. Several strategies, such as use of dopants, metal dispersion, carbon coating and co-synthesizing the phosphate with carbon have thus been implemented by number of groups [2,3,6–22]. Yamada et al., for example, have shown that the control of the particle size through control of the annealing temperatures with addition of carbon is crucial for assuring the high performance of the $LiFePO_4$ cathode material [23]. On the other hand, Chung et al. reported that the electronic conductivity of $LiFePO_4$ could be enhanced by a factor of $\sim 10^8$ (10^{-2} S cm^{-1}) by doping supervalent cations delivering specific capacity of ≈140 mAh g^{-1} at *C*/10 rate [6,24]. However, Nazar and co-workers subsequently reported that such an improvement in electronic conductivity was possibly attributed to the formation of iron phosphide during high temperature (>600 °C) heat-treatment [25]. These results have spurred a debate regarding the need for some conducting phase or additive to improve the conductivity of $LiFePO_4$. Alternatively, Armand and co-workers showed improvements in the kinetics of the electrochemical reaction by coating electronically conducting carbon on the $LiFePO_4$ particles during synthesis in which almost the full theoretical capacity was achieved at 80 °C [7,26,27].

The $LiFePO_4$ cathode is affected by a loss in capacity with increasing current density, associated with diffusion-controlled

* Corresponding author at: Department of Materials Science and Engineering, 4309 Wean Hall, 5000 Forbes Avenue Carnegie Mellon University, Pittsburgh, PA 15213, United States.
E-mail address: kumta@cmu.edu (P.N. Kumta).

0378-7753/$ – see front matter © 2006 Elsevier B.V. All rights reserved.
doi:10.1016/j.jpowsour.2006.09.082

kinetics of the electrochemical process. Efforts to bypass the above-mentioned kinetic limitations may involve synthesizing the material at medium–high temperature or enhancing its ionic/electronic conductivity by developing innovative low temperature routes to synthesize $LiFePO_4$. Previous studies clearly indicate the critical importance of $LiFePO_4$ particle morphology to overcome the poor electronic and ionic conductivity limitations. Although the Li^+ ion diffusion in the olivine structure is proven to be primarily one-dimensional along the *b*-axis, modeling studies based on the shrinking core model did indicate the strong correlation of smaller particle size affecting the rate capability of $LiFePO_4$ [28,29]. Recently, carbon free $LiFePO_4$ with a narrow particle size distribution (average particle size: ≈140 nm) synthesized by aqueous precipitation delivered 140 mAh g^{-1} at 10*C* rate [30,31]. In addition, various sol–gel routes [32–35] and a low temperature polyol process has also been successfully utilized for synthesizing nanosized (20–40 nm) $LiFePO_4$ with improved electrochemical response [36].

In this current study, we report enhancing the electrochemical performance of the $LiFePO_4$ electrode by controlling the particle morphology via a nonaqueous sol–gel process using lauric acid as a surfactant. Such a surfactant based sol–gel technique applied for obtaining high surface area mesoporous alumina oxides offers a novel, simple, cheap and a robust way to prepare $LiFePO_4$ [37]. The present paper provides a detailed account of the material synthesis, characterization and its electrochemical response.

2. Experimental

2.1. Synthesis and material characterization

Olivine-type $LiFePO_4$ was synthesized using $CH_3CO_2Li\cdot 2H_2O$ (>98%, Aldrich), $FeCl_2\cdot 4H_2O$ (>99%, ACROS) and P_2O_5 (Reagent ACS, ACROS) precursors. Each precursor was dissolved separately in ethanol (200 Proof, 99%, Pharmco) to yield a 1 M solution. The Fe and P solution was first mixed in the desired stoichiometric ratio and stirred for 3 h followed by the addition of stoichiometric amount of the Li solution. Equal molar ratio of lauric acid (98%, ACROS) surfactant was added to the solution after 3 h of stirring. After 4 h, the reaction was presumed to be complete and the ethanol was evaporated under continuous flow of ultra high purity (UHP)-Ar followed by heat-treatment under H_2/Ar = 10%/90% atmosphere at 500 °C for 5 h (flow rate: 120 cm^3 min^{-1}, heating rate: 1 °C min^{-1}) to prevent the possible formation of Fe^{3+} impurities. $LiFePO_4$ without lauric acid was also synthesized to compare the effect of the surfactant on the resultant electrochemical response. The obtained $LiFePO_4$ powder was subjected to X-ray diffraction (X'pert Pro, Philips) for phase analysis using Cu Kα radiation (λ = 1.5418 Å) scanned in the 10–90° range with a step size of 0.0334 and a 50 s exposure time. The lattice parameters were determined by Rietveld refinement using the X'pert plus (Philips) while the average crystallite size was calculated by the Scherrer equation from the full width at half maximum (FWHM) of (0 1 1), (1 1 1) or (0 2 1), (1 2 1) or (2 0 0), (1 3 1) peaks using the Profit software (Philips). The specific surface areas of the synthesized $LiFePO_4$ were measured using the multi-point (8) Brunauer–Emmett–Teller (BET) technique (Quantachrome Inst., NOVA-2000).

The morphology of the $LiFePO_4$ powder was observed by scanning electron microscopy (SEM, Phillips XL 30 FEG SEM) and the particle size distribution was calculated by inserting lines across the images and measuring the distance between the start and end of the grain boundaries of 300 particles. High-resolution transmission electron microscopy (HRTEM, Philips Tecnai 20 FEG) was also used to observe the morphology and particle size whereas surface elemental analysis was conducted using energy dispersive X-ray (EDX) analysis. For HRTEM observation, the $LiFePO_4$ powders were dispersed on 3.05 mm diameter copper grids (electron microscopy science) containing a holey carbon film in methanol by sonication followed by drying under vacuum for 24 h. The carbon content was determined by Luvak Inc. (Boylston, MA) using the combustion infrared detection method. The electronic conductivity was measured on the compacted $LiFePO_4$ powder pellet (uniaxial pressure of 7000 lb) using the four-point probe method comprised of 3-D adjustable probes and a digital source meter (Keithley 2400).

2.2. Electrochemical characterization

For electrochemical evaluation, the cathode comprised of active material, super P and poly(vinylidene fluoride) (PVDF) binder were dispersed in *N*-methylpyrrolidone (NMP) solution in a weight ratio of 85:10:5, respectively. The slurry was then coated on the aluminum metal foil current collector and dried overnight in air. The active materials loading on the cathode was between 2 mg and 2.5 mg on 0.95 cm^2 current collector area. The performance of the $LiFePO_4$ cathode was evaluated using Arbin Inst. (College Station, TX) on Hockey-puck-type (half-cell) configuration at room temperature. The cells were tested between 4.5 V and 2.0 V versus Li metal at various rates (10*C* to *C*/10). The electrolyte used was 1 M $LiPF_6$ dissolved in propylene carbonate (PC) solution employing lithium metal as both the reference and the anode electrode.

3. Results and discussion

Fig. 1 shows the XRD pattern of the $LiFePO_4$ powder synthesized using lauric acid at 500 °C under $10H_2$/90Ar atmosphere. Based on space group *Pnma*, the lattice constants of $a = 10.3297$ Å, $b = 6.0056$ Å and $c = 4.6908$ Å were obtained by Rietveld refinement analysis indicating a highly crystalline stoichiometric $LiFePO_4$ phase (JCPDS 81-1173, *Pnma*(62), $a = 10.33$ Å, $b = 6.010$ Å, $c = 4.692$ Å). The crystallite size (*D*) was calculated from the Scherrer equation $\beta\cos(\theta) = k\lambda/D$, where β is the full-width-at-half-maximum (FWHM) of the XRD peak and *k* is a constant (0.9). The mean crystallite size *D* of the $LiFePO_4$ decreased from 64.01 ± 5.3 nm to 51.03 ± 0.8 nm whereas the specific surface area increased from 7.5 m^2 g^{-1} to 36.7 m^2 g^{-1} when lauric acid was added during the synthesis. The pore size distribution was obtained from the desorption isotherm based on the Barret–Joyner–Halenda (BJH) method where most of the pores were within the mesopore region

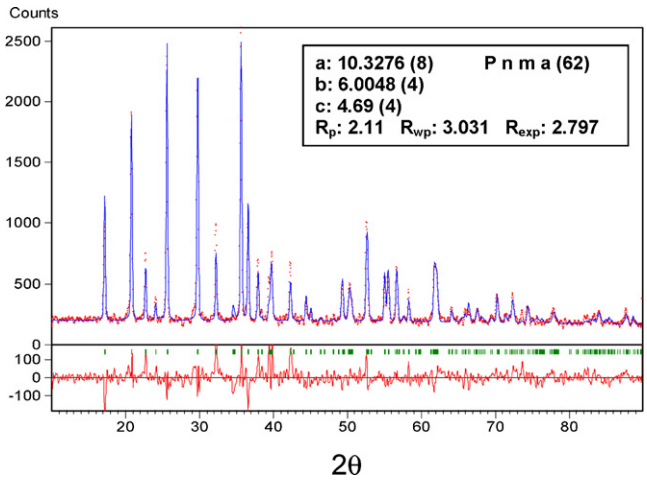

Fig. 1. Rietveld refinement on the XRD pattern of $LiFePO_4$ synthesized using lauric acid at 500 °C under $10H_2$–90Ar atmosphere.

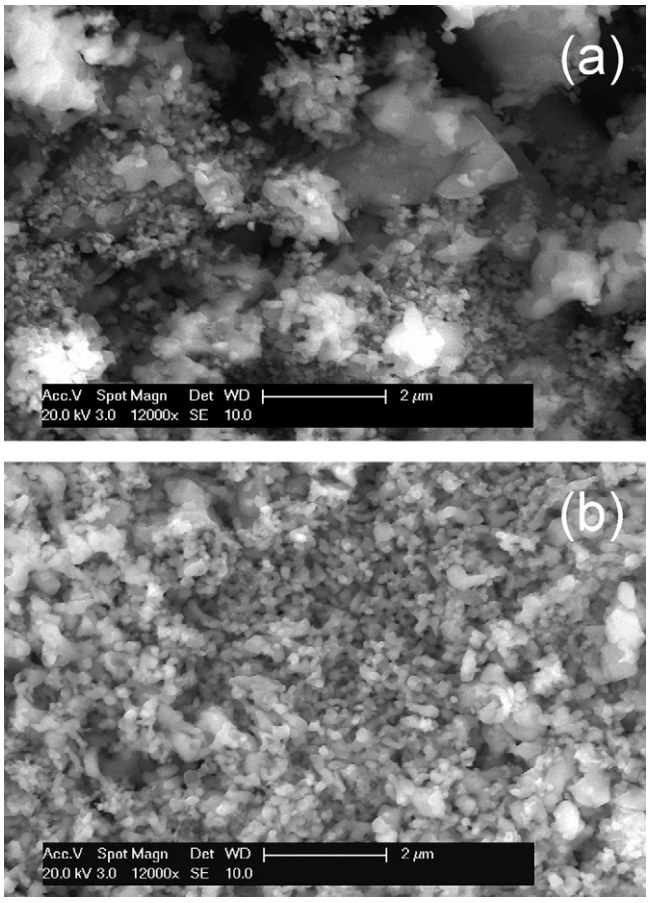

Fig. 2. The SEM micrographs of $LiFePO_4$ powders synthesized (a) without and (b) with lauric acid after heat-treatment of the precursor at 500 °C under $10H_2$–90Ar atmosphere.

(2–50 nm). The addition of lauric acid increased the residual carbon content from 0.81 wt.% to 4.18 wt.%. However, the electronic conductivity measured on the $LiFePO_4$ pellet synthesized with and without the surfactant were 1.55×10^{-9} S cm^{-1} and 1.44×10^{-9} S cm^{-1} at room temperature, respectively. These values are comparable to that of pure $LiFePO_4$ and the negligible difference in electronic conductivity suggests the non-conducting behavior of the carbonaceous residue present in the $LiFePO_4$ powder. Furthermore, the electronic conductivities being similar to that of pure $LiFePO_4$ indicate the absence of the Fe_2P impurity phase ($P\bar{6}2m$; 5.2×10^{-2} S cm^{-1}) in the phosphate synthesized with and without surfactant. The Fe_2P phase has been implicated to increase the electronic conductivity of $LiFePO_4$ when carbon containing precursors were used [25]. If Fe_2P were to form in the present approach, XRD and HRTEM–EDX analysis would detect the presence of the phosphide. The XRD results indicate no traces of the strongest (1 1 1) peak corresponding to the phosphides near 2θ angles in the range of 40.28–42.39° [20]. HRTEM–EDX analyses have also been conducted as described later, which validates the absence of the Fe_2P phase confirming that the electronic conductivities of the two phosphates arise from the $LiFePO_4$ phase and not from any impurity phases.

Fig. 2 shows the SEM micrographs of the $LiFePO_4$ powders synthesized with and without surfactant at 500 °C. It has been reported that the particle growth is inhibited when the phosphate is synthesized below 600 °C [16]. The SEM micrographs clearly show the difference in microstructure of the $LiFePO_4$ powder synthesized in the presence of lauric acid. The $LiFePO_4$ synthesized without surfactant contains particles of various sizes ranging from few hundred of nanometers to several microns whereas the $LiFePO_4$ synthesized with the surfactant shows uniform nanometer-sized (~170 nm) particles interconnected to form a porous network. Particle size distributions of $LiFePO_4$ powders were estimated based on the SEM micrographs as shown in Fig. 3. The relative span of the particle size distribution (PSD) defined as $(D_{90} - D_{10})/D_{50}$ decreased from 3.1 to 1.1 when the surfactant was used during the synthesis. This shows that approximately 80% of $LiFePO_4$ is within 100–300 nm range with an average particle size of ≈170 nm compared to that of ≈600 nm corresponding to the $LiFePO_4$ synthesized without the surfactant. These results therefore show that the surfactant based sol–gel approach is suitable for obtaining stoichiometric $LiFePO_4$ powder with effectively controlled particle size and porosity.

To identify the possible existence of impurity phases such as Fe_2P, HRTEM coupled with EDX analyses in the STEM mode were undertaken across the surfaces of the $LiFePO_4$ powder obtained at 500 °C using the surfactant, the results of which are shown in Fig. 4. The observation of near stoichiometric $LiFePO_4$ with average Fe/P atomic ratio of 1.09 ± 0.13 ($n = 10$) determined by EDX analysis from the particle core to the surface clearly indicates the absence of any iron phosphide layer around the particles. However, traces of carbon (5.19 wt.%) and chlorine (0.32 wt.%) residue have been also detected by the EDX analysis which is possibly arising from the precursors used. The carbon analysis is in good agreement with the chemical analysis results. This strengthens the results of the XRD and electronic conductivity analyses suggesting that the electrical conductivity was comparable to that of pure $LiFePO_4$ reported.

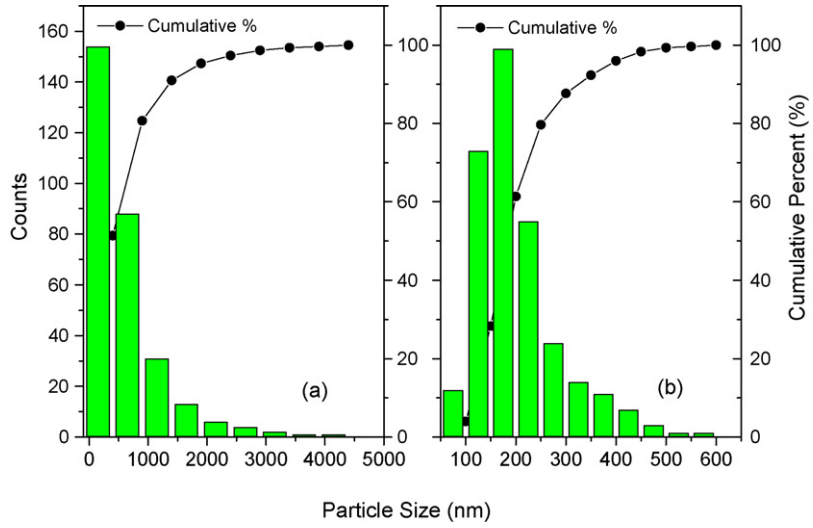

Fig. 3. Particle size distribution of $LiFePO_4$ powders synthesized (a) without and (b) with lauric acid after heat-treating the precursor at 500 °C under $10H_2$–90Ar atmosphere.

Fig. 5 shows the galvanostatic discharge curves of the $LiFePO_4$ cathodes measured at different rates starting from *C*/10 to 10*C* rate between 4.5 V and 2.0 V versus Li. The $LiFePO_4$ synthesized with surfactant exhibited significantly better electrochemical performance with a specific capacity of 170 mAh g^{-1}, the theoretical limit at *C*/10 rate. In contrast, the $LiFePO_4$ synthesized without surfactant yielded only 146 mAh g^{-1} at *C*/10 and did not show much improvement even at lower *C* rates. We believe this is due to presence of large particles which cannot be fully utilized to the core of the particle. At 5*C* rate, specific capacity of 90 mAh g^{-1} was recorded for $LiFePO_4$ synthesized without lauric acid, which is comparable to other $LiFePO_4$ containing a carbon coating (≈10 wt.%) or metal dopants reported by Striebel et al. [38]. However, when the surfactant was used, a specific capacity of 142 mAh g^{-1} and 125 mAh g^{-1} was delivered at 5*C* and 10*C* rate, respectively. Such a significant improvement in the electrochemical kinetics of the $LiFePO_4$ powder is believed to be caused by the improved surface area, reduced par-

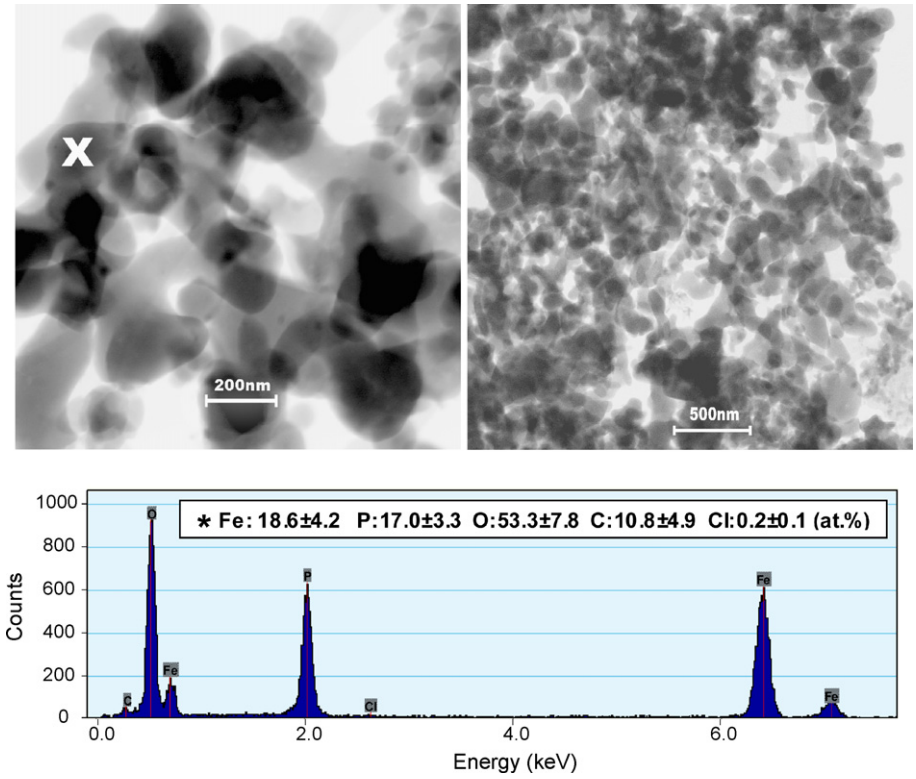

Fig. 4. HRTEM image and EDX spectra of $LiFePO_4$ powders synthesized with lauric acid after heat-treatment of the precursor at 500 °C under $10H_2$–90Ar atmosphere. (X) Area selected for EDX analysis and (*) average composition from $n = 10$.

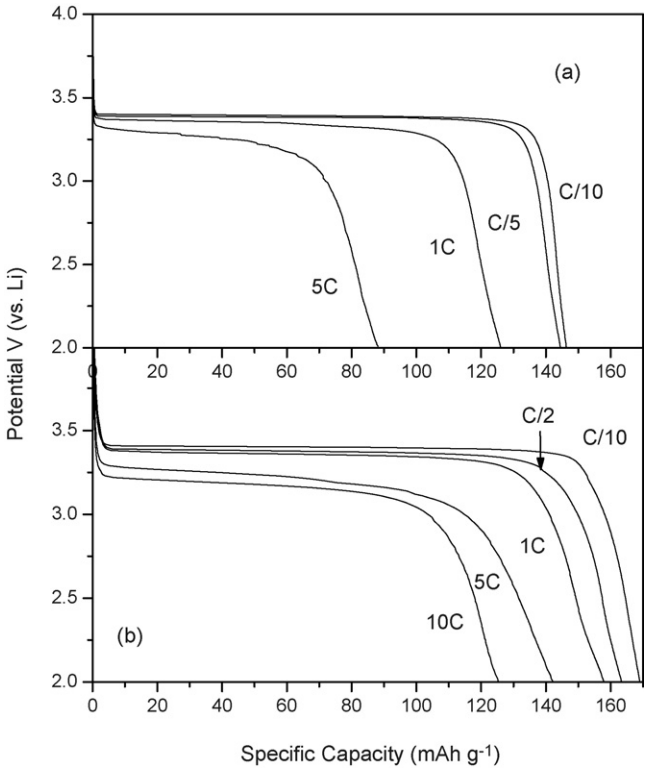

Fig. 5. The voltage profile recorded during discharge vs. specific capacity at different *C* rates for $LiFePO_4$ synthesized (a) without and (b) with lauric acid.

ticle size and the porous structure of the phosphate. The higher specific surface area along the *a*–*c*-axis plane and a narrow distribution of nanosized particles would tend to offset the barriers to high rates governed by both the poor intrinsic electronic and ionic conductivity of the phosphates [28–30]. The electronic diffusion coefficient in the olivine $LiFePO_4$ cathode is reported to be 8×10^{-18} m^2 s^{-1} whereas the Li^+ diffusion coefficient in the $LiFePO_4$ and $FePO_4$ phases was found to be 1.8×10^{-18} m^2 s^{-1} and 2.2×10^{-20} m^2 s^{-1}, respectively [39]. Since the Li^+ ion and electronic conductivities are in the same range of magnitude, it is important to shorten both electronic and ionic paths within the particles [39,40]. If the particle size is widely distributed as is the case of $LiFePO_4$ obtained without the surfactant, the small particles will fill/deplete up faster than the larger ones during discharge/charge reaction and the $LiFePO_4$ near the center of the larger particle will thus contribute very little to the redox reaction. In addition, it is also necessary to create a porous structure in order to realize unhindered transport of electrolyte into the particle's exterior [17,19].

It should be also noted that the constant voltage profile (dq/dv peak potential) of the discharge curve dropped from 3.37 V to 3.3 V as the rate increased from *C*/2 to 5*C* irrespective of how the $LiFePO_4$ was prepared due to the contact and matrix resistance related to the limited electronic conductivity of the phosphate [29]. However, the discharge voltage profile of $LiFePO_4$ obtained with surfactant was quite steady and constant even at 5*C* and 10*C* rate indicating that the resistance to ionic diffusion is small [29]. Typically, during discharge, the smaller particles accept Li^+ faster and a mismatch in the degree of charged states

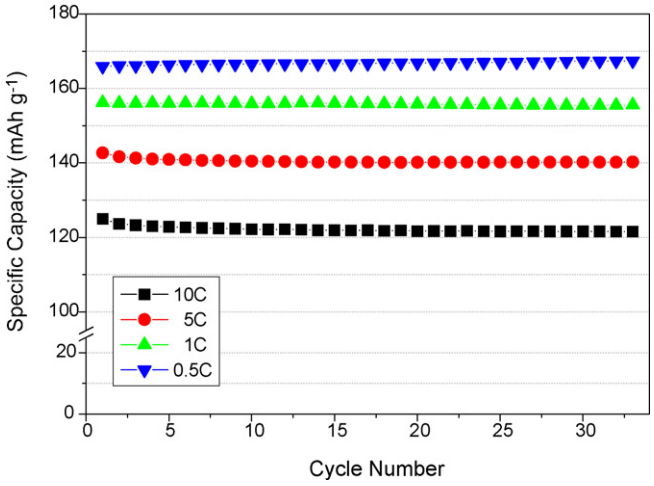

Fig. 6. The discharge specific capacity retention *vs.* the cycle number for $LiFePO_4$ nanocrystallites synthesized with lauric acid at 500 °C under $10H_2$–90Ar atmosphere scanned between 10*C* and *C*/2 up to 33 cycles.

results in a larger over-potential for the smaller particles compared to the larger ones due to a greater change in the equilibrium potential, thereby allowing the larger particles to subsequently catch up. However, in the case of olivine-type $LiFePO_4$, the relatively flat potential of the two-phase $LiFePO_4/FePO_4$ transition does not allow significant mismatch among particles with different sizes until the smaller particle is completely utilized. The lack of apparent change in the slope of the voltage profile for $LiFePO_4$ obtained using lauric acid validates the uniform and nanosized nature of the $LiFePO_4$ particles.

Fig. 6 shows the cycling behavior at different *C*-rates of $LiFePO_4$ synthesized with lauric acid at different charge rates. At all rates, good cycling capabilities of $LiFePO_4$ can be observed with less than 0.083% $cycle^{-1}$ decrease in specific capacity between the 1st and the 33rd cycle. The cycling performance improved after the 10th cycle with 0.022% $cycle^{-1}$ decrease between the 10th and the 33rd cycle. These excellent cycling characteristics combined with improved kinetics of $LiFePO_4$ confirm the role of optimizing the particle size and porosity of the $LiFePO_4$ electrode material synthesized using lauric acid as the surfactant. Also, improvement in electronic conductivity through effective carbon coating could further improve the rate capability. As a continuation of the current study, the effect of various types of carboxylic acids on the microstructure and electrochemical performance is being studied and will be reported subsequently.

4. Conclusion

Nanostructured $LiFePO_4$ powder was prepared by a sol–gel method using lauric acid as the surfactant. The $LiFePO_4$ synthesized with the surfactant delivered a specific capacity of 125 mAh g^{-1} and 157 mAh g^{-1} at discharge rates of 10*C* and 1*C*, respectively, which is a significantly better rate performance compared to the phosphate obtained without any surfactant. These results show that the rate performance of $LiFePO_4$ cathode can be enhanced by changing the particle size and porosity

of $LiFePO_4$ particles. The major advantage of the current sol–gel approach is the formation of a porous networked structure with uniform particle size by utilizing a carboxylic acid surfactant, which acts as a capping agent preventing and minimizing the agglomeration of the phosphate particles.

Acknowledgement

This work was supported in part by the National Science Foundation (Grant CTS-0000563).

References

[1] N. Terada, T. Yanagi, S. Arai, M. Yoshikawa, K. Ohta, N. Nakajima, N. Arai, J. Power Sources 1–2 (2001) 80–92.
[2] J. Shim, K.A. Striebel, J. Power Sources 119–121 (2003) 955–958.
[3] K.A. Striebel, A. Guerfi, J. Shim, M. Armand, M. Gauthier, K. Zaghib, J. Power Sources 119–121 (2003) 951–954.
[4] A.K. Padhi, K.S. Najundaswamy, J.B. Goodenough, J. Electrochem. Soc. 144 (1997) 1188–1194.
[5] A.S. Andersson, B. Kalska, L. Häggström, J.O. Thomas, Solid State Ionics 130 (2000) 41–52.
[6] S.-Y. Chung, J.T. Bloking, Y.-M. Chiang, Nat. Mater. 2 (2002) 123–128.
[7] H. Huang, S.-C. Yin, L.F. Nazar, Electrochem. Solid-State Lett. 4 (2001) A170–A172.
[8] S. Yang, Y. Song, P.Y. Zavalij, M.S. Whittingham, Electrochem. Commun. 4 (2002) 239–244.
[9] J. Barker, M.Y. Saidi, J.L. Swoyer, Electrochem. Solid-State Lett. 6 (2003) A53–A55.
[10] M.M. Doeff, Y. Hu, F. McLarnon, R. Kosteckl, Electrochem. Solid-State Lett. 6 (2003) A207–A209.
[11] Z. Chen, J.R. Dahn, J. Electrochem. Soc. 149 (2002) A1184–A1189.
[12] H. Gabrisch, J.D. Wilcox, M.M. Doeff, Electrochem. Solid-State Lett. 9 (2006) A360–A363.
[13] F. Croce, A.D. Epifanio, J. Hassoun, A. Deptula, T. Olczac, B. Scrosati, Electrochem. Solid-State Lett. 5 (2002) A47–A50.
[14] G.X. Wang, L. Yang, Y. Chen, J.Z. Wang, S. Bewlay, H.K. Liu, Electrochem. Acta 50 (2005) 4649–4654.
[15] G.X. Wang, S.L. Bewlay, K. Konstantinov, H.K. Liu, S.X. Dou, J.-H. Ahn, Electrochem. Acta 50 (2004) 443–447.
[16] X.-Z. Liao, Z.-F. Ma, Y.-S. He, X.-M. Zhang, L. Wang, Y. Jiang, J. Electrochem. Soc. 152 (2005) A1969–A1973.
[17] R. Dominko, J.M. Goupil, M. Bele, M. Gaberseek, M. Remskar, D. Hanzel, J. Jamnik, J. Electrochem. Soc. 152 (2005) A843–A858.
[18] G.X. Wang, L. Yang, S.L. Bewlay, Y. Chen, H.K. Liu, J.H. Ahn, J. Power Sources 146 (2005) 521–524.
[19] M. Takahashi, S. Tobishima, K. Takei, Y. Sakurai, J. Power Sources 97–98 (2001) 508–511.
[20] G. Arnold, J. Garche, R. Hemmer, S. Strobele, C. Vogler, M. Wohlfahrt-Mehrens, J. Power Sources 119–121 (2003) 247–251.
[21] A.D. Spong, G. Vitins, J.R. Owen, J. Electrochem. Soc. 152 (2005) A2376–A2382.
[22] Y. Hu, M.M. Doeff, R. Kostecki, R. Finones, J. Electrochem. Soc. 151 (2004) A1279–A1285.
[23] A. Yamada, S.C. Chung, K. Hinokuma, J. Electrochem. Soc. 148 (2001) A224–A229.
[24] S.Y. Chung, Y.M. Chiang, Electrochem. Solid-State Lett. 6 (2003) A278–A281.
[25] P. Subramanya Herle, B. Ellis, N. Coombs, L.F. Nazar, Nat. Mater. 3 (2004) 147–152.
[26] N. Ravet, S. Besner, M. Simoneau, A. Vallée, M. Armand, Hydro-Québec, Canadian Patent 2,270,771.
[27] N. Ravet, J.B. Goodenough, S. Besner, M. Simoneau, P. Hovington, M. Armand, Abstract 127, The 196th Electrochemical Society and the Electrochemical Society of Japan Meeting Abstracts, vol. 99–102, Honolulu, HI, October 17–22, 1999.
[28] G. Chen, X. Song, T.J. Richardson, Electrochem. Solid-State Lett. 9 (2006) A295–A298.
[29] V. Srinivasan, J. Newman, J. Electrochem. Soc. 151 (2004) A1517–A1529.
[30] C. Delacourt, P. Poizot, S. Levasseur, C. Masquelier, Electrochem. Solid-State Lett. 9 (2006) A352–A355.
[31] C. Delacourt, P. Poizot, M. Morcrette, J.-M. Tarascon, C. Masquelier, Chem. Mater. 16 (2004) 93–99.
[32] R. Dominko, M. Bele, M. Gaberscek, M. Remskar, D. Hanzel, J.M. Goupil, S. Pejovnik, J. Jamnik, J. Power Sources 153 (2006) 274–280.
[33] J.S. Yang, J.J. Xu, J. Electrochem. Soc. 153 (2006) A716–A723.
[34] M.A.E. Sanchez, G.E.S. Brito, M.C.A. Fantini, G.F. Goya, J.R. Matos, Solid State Ionics 177 (2006) 497–500.
[35] Z.P. Guo, H. Liu, S. Bewlay, H.K. Liu, S.X. Dou, J. New Mater. Electrochem. Syst. 6 (2003) 259–262.
[36] D.-H. Kim, J. Kim, Electrochem. Solid-State Lett. 9 (2006) A439–A442.
[37] F. Vaudry, S. Khodabandeh, M.E. Davis, Chem. Mater. 8 (1996) 1451–1464.
[38] K. Striebel, J. Shim, V. Srinivasan, J. Newman, J. Electrochem. Soc. 1524 (2005) A664–A670.
[39] P.P. Prosini, M. Lisi, D. Zane, M. Pasquali, Solid State Ionics 148 (2002) 45–51.
[40] S. Franger, F. Le Cras, C. Bourbon, H. Rouault, Electrochem. Solid-State Lett. 5 (2002) A231–A233.